Resumption of dynamism in damaged networks of coupled oscillators

Srilena Kundu, Soumen Majhi, and Dibakar Ghosh
Physics and Applied Mathematics Unit, Indian Statistical Institute, 203 B. T. Road, Kolkata 700108, India

(Received 17 November 2017; revised manuscript received 8 May 2018; published 31 May 2018)

Deterioration in dynamical activities may come up naturally or due to environmental influences in a massive portion of biological and physical systems. Such dynamical degradation may have outright effect on the substantive network performance. This requires us to provide some proper prescriptions to overcome undesired circumstances. In this paper, we present a scheme based on external feedback that can efficiently revive dynamism in damaged networks of active and inactive oscillators and thus enhance the network survivability. Both numerical and analytical investigations are performed in order to verify our claim. We also provide a comparative study on the effectiveness of this mechanism for feedbacks to the inactive group or to the active group only. Most importantly, resurrection of dynamical activity is realized even in time-delayed damaged networks, which are considered to be less persistent against deterioration in the form of inactivity in the oscillators. Furthermore, prominence in our approach is substantiated by providing evidence of enhanced network persistence in complex network topologies taking small-world and scale-free architectures, which makes the proposed remedy quite general. Besides the study in the network of Stuart-Landau oscillators, affirmative influence of external feedback has been justified in the network of chaotic Rössler systems as well.

DOI: 10.1103/PhysRevE.97.052313

I. INTRODUCTION

Network theory offers an excellent platform to understand the universal properties of many natural and engineered systems made up of a large number of units. Study of emergent collective behaviors in large ensembles of coupled dynamical units has received enormous appreciation because of its intensive applicability in imitating various self-organized complex systems [1,2]. Among other perspectives, one which deals with the exploration of network robustness (i.e., the ability to withstand perturbations) has extensive importance from several aspects. This scenario can be thought of in two different ways: *topological robustness* [3–11] and *dynamical robustness* [12–20,28,29]. The first one discusses the persistence of network activities against structural perturbations in the form of removal of links (bond percolation) or nodes (site percolation) in the network. In this context, one of the most fundamental results demonstrates that the heterogeneous scale-free structures exhibit high resilience against random failure in the nodes whereas random networks are much less robust and the diameter of the network increases monotonically. But, scale-free networks are vulnerable to targeted attacks, while for random connection topology there is no significant change in the way of attacking owing to the homogeneity in the degree distribution [3,5]. In contrast, for two interdependent networks, broader degree distribution (like that in scale-free structure) is much more sensitive to random failures [6,8].

On the other hand, another exploration of robustness is concerned with the network's survivability with respect to local perturbations in the dynamical activities of the nodes. This can be realized by exploring the evolution patterns of damaged networks made up of mixed populations comprising active (healthy) and inactive (ill) dynamical units, known as *aging transition* (AT) [12] in the literature. In fact, there exist several instances in ecological networks [21–23], where some patches in the metapopulation become extinct, that may have dramatic effects on the underlying developments. In neuronal networks, it is the rhythmicity of the neurons that governs the possibility of information exchange among them. So, loss in activity of a neuron may have several unexpected consequences [24]. Moreover, for appropriate functioning in cardiac and respiratory systems [25], and specific physiological processes [26], for instance cell necrosis within organs [27], robust global oscillation is quite necessary. The study of dynamical robustness has also been extended to a network of complex topology [28] and a power grid network [29] where the failure of a node is modeled via injecting noise into the dynamics of that node.

But despite high relevance the possible remedies to overcome the comprehensive dynamical failure of the network and hence to resurrect dynamism are yet to be fully explored and deserve significant consideration. The existing researches rather mainly focused on the issue of aging transition under various interactional topologies of the network or using different coupling functions. For instance, such transitions are explained in globally [12,13] and locally [14] coupled networks and in multilayer [15] networks as well. The crucial role of the low degree nodes in a scale-free network [17] has also been discussed. Time delay in the interactions may lower the network resilience under aging [16]. Nevertheless, Liu *et al.* [19] put forward the notion of an additional parameter that controls the diffusion rate in order to enhance network persistence. Network robustness can also be developed by bringing uniform and normal random errors into the distance parameters of the system [20]. In [18], authors rendered a mechanism of recovering dynamical behavior in aging networks by additionally connecting supporting oscillators to the network. But adding intact oscillators in the network increases

the effective size of the network. In the current paper, we present an adaptable mechanism that involves introduction of external feedback in resurging dynamical activity in the network and hence development of network survivability, for which one does not need to change the intrinsic parameters of the system or to increase the effective network size.

The concept of feedback is considered as one of the most important scientific understandings and as the heart of control theory [30,31]. Particularly, positive feedback has been found to have colossal importance in natural systems [32] having impacts in evolutionary processes, physical systems, organism physiology, social evolution, ecosystems, and many more. It is also used in genetic networks [33], neuronal networks [34,35], etc. In fact, positive feedback has been found to favor system instability in dynamical systems and is utilized in elevating chaotic behavior and diverging from equilibrium, a scenario that we will be exploring in this paper as well. As far as the synchronization and control of networked dynamical systems are concerned, utility of feedback has been well justified [36–45]. But, the influence of that entity in damaged networks of active (healthy) and inactive (diseased) dynamical systems is yet to be given attention, which is the focus of the present paper. We put forward a detailed study on the ability of external positive feedback to improve the network survivability while the network is experiencing aging transition. We present analytical results on this issue that perfectly match the numerical ones. As discussed earlier [16], time-delayed interaction among the systems may lower the network's persistence against local inactivation of the dynamical units. Here we show that even under this situation feedback is a mechanism that is quite capable in enhancing network robustness. In addition, we explore this in complex topologies, such as small-world and scale-free networks, that makes our idea independent of network architecture. To demonstrate that our scheme is not system dependent, we provide results on both the Stuart-Landau limit cycle system and chaotic Rössler oscillator.

This paper is organized as follows. In Sec. II, we provide a brief description of the network model of coupled Stuart-Landau oscillators. The general mathematical form of the network for globally interacting oscillators is provided in Sec. III. Numerical results followed by analytical study for globally interacting the nondelay and delay coupled network are illustrated in Secs. III A and IIIB, respectively. We show the effect of feedback in complex network topologies in Sec. IV. Section IVA deals with the results in the case of the small-world network, whereas the results for the scale-free network are summarized in Sec. IV B. Section V is devoted to the analysis of networked Rössler systems. Finally, Sec. VI offers concluding remarks on the obtained results.

II. MODEL DESCRIPTION OF THE DAMAGED NETWORK OF COUPLED STUART-LANDAU OSCILLATORS

We consider the following network model of N nodes as

$$\dot{z}_j = \mathbf{F}(z_j) + \frac{\epsilon}{N}\sum_{k=1}^{N} A_{jk}(z_k - z_j) + \eta f(\bar{z}), \qquad (1)$$

for $j = 1,2,\ldots,N$ where $\mathbf{F}: \mathbb{R}^m \to \mathbb{R}^m$ represents the vector field corresponding to the system evolution whereas the function $f: \mathbb{R}^m \to \mathbb{R}^m$ defines the external feedback term. A_{jk} is the adjacency matrix characterizing the connectivity pattern of the network, i.e., $A_{jk} = 1$ if jth and kth nodes are connected and zero otherwise. The parameters ϵ and η, respectively, account for the direct diffusive interaction strength and the strength of the feedback.

Here we start by taking local dynamical units as the Stuart-Landau oscillators in the form

$$\mathbf{F}(z_j) = (\alpha_j + i\omega - |z_j|^2)z_j, \qquad (2)$$

for $j = 1,2,\ldots,N$ where α_j are the internal parameters of the jth system that define the distance from a Hopf bifurcation, ω is the natural frequency of oscillation, and $i = \sqrt{-1}$. In isolation, the jth unit displays a stable limit cycle $\sqrt{\alpha_j}e^{i\omega t}$ if $\alpha_j > 0$ and settles into the stable trivial fixed point $z_j = 0$ for $\alpha_j \leqslant 0$. As a result of this, active and inactive oscillators in the network, respectively, possess $\alpha_j = a > 0$ and $-b < 0$. For the present paper, we have chosen the external feedback to be linear of the form $f(\bar{z}) = \bar{z} = \frac{1}{N}\sum_{k=1}^{N} z_k$ (a nonlinear feedback function could make the system more complicated without any additional advantage; in fact this simple linear form is quite effective, as we have shown later).

Next we follow the procedure in [12] that defines the inactivation ratio (ratio of non-self-oscillatory elements) p, which is the ratio of the number of inactive nodes and the total number of nodes in the network. Whenever p exceeds a certain critical value p_c (say), the global oscillation of the network dies out. So, our aim will be to restrain this sort of phase transition while utilizing the feedback parameter (η), as long as possible. We will explore the scenario of aging transition arising in the network in terms of the normalized order parameter $Z = \frac{|\bar{z}(p)|}{|\bar{z}(0)|}$, so that $|\bar{z}|$ identifies the intensity of global oscillation in the networked system and Z is the normalized value of it. We have fixed the network size $N = 500$ (however, all the results are tested for larger networks). Without loss of generality, $a = 2$, $b = 1$, and $\omega = 3$ are considered throughout the paper [46].

III. GLOBALLY COUPLED NETWORK

In this section, we present a comprehensive study on the effect of feedback parameter to enhance dynamical robustness in the presence or absence of time-delayed interaction, while considering network of globally coupled oscillators. Then the mathematical form of the network reads as

$$\dot{z}_j = (\alpha_j + i\omega - |z_j|^2)z_j + \frac{\epsilon}{N}\sum_{k=1,k\neq j}^{N}[z_k(t-\tau) - z_j] + \frac{\eta}{N}\sum_{k=1}^{N} z_k, \qquad (3)$$

where τ refers to the time delay in the direct interactions among the nodes. For the sake of simplicity, we set the group of active elements as $j \in \{1,2,\ldots,N - Np\}$ and that of the inactive elements as $j \in \{N - Np + 1,\ldots,N\}$.

A. Nondelayed interaction

Whenever there is no time delay, i.e., with $\tau = 0$, the network (3) reduces to Eq. (1) along with Eq. (2). But before going into the details of this we first analyze the evolution in

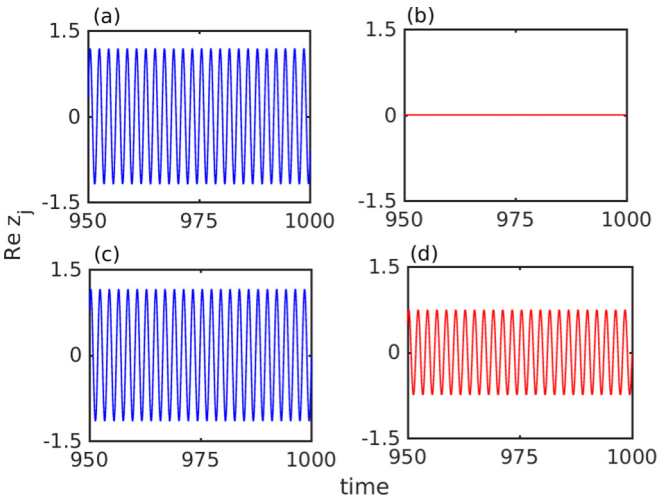

FIG. 1. The dynamics of N completely synchronized globally coupled Stuart-Landau oscillators in (a) active state, i.e., when $p = 0$, and (b) inactive state, i.e., when $p = 1$. The behavior of (c) $(1-p)N$ active and (d) pN inactive oscillators corresponding to the inactivation ratio $p = 0.2$. Here, coupling strength $\epsilon = 3$ and feedback parameter $\eta = 0$.

the dynamics of the oscillators before and after the inactivation procedure. The dynamics of N globally coupled synchronized Stuart-Landau oscillators for nonzero interaction strength, particularly for $\epsilon = 3$ (with $\eta = 0$), is depicted in Fig. 1, which is of limit cycle type with amplitude $\sqrt{2}$ for the active state (i.e., $p = 0$), while in the inactive state (i.e., $p = 1$) the nodes are stable at the trivial fixed point, i.e., the origin. The respective real parts of z_j, i.e., $\mathrm{Re}(z_j)$, are shown in Figs. 1(a) and 1(b). But considering a specific $p = 0.2$ (i.e., when 20% of the nodes are in the inactive state) the inactive nodes start oscillating, relying on the influence of the active nodes, which is depicted through $\mathrm{Re}(z_j)$ in Figs. 1(c) and 1(d).

Figure 2 shows the variation in Z with respect to the increasing inactivation ratio p $(0 \leqslant p \leqslant 1)$ for different values

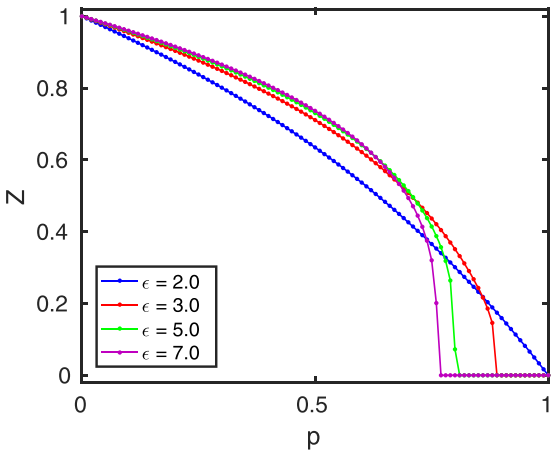

FIG. 2. The order parameter Z vs the inactivation ratio p corresponding to various coupling strengths $\epsilon = 2,3,5$, and 7 without feedback parameter $(\eta = 0)$. The critical inactivation ratio p_c decreases gradually as ϵ increases.

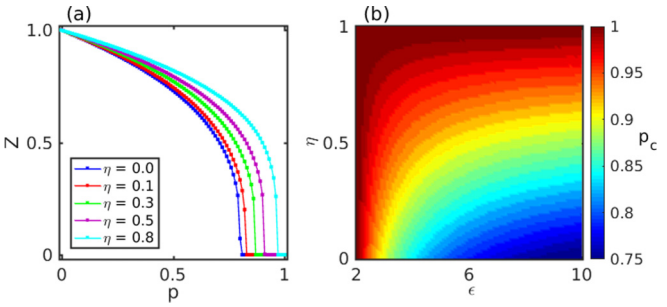

FIG. 3. (a) The order parameter Z against the inactivation ratio p corresponding to coupling strength $\epsilon = 5$ and various feedback parameter values $\eta = 0,0.1,0.3,0.5$, and 0.8. As η increases p_c value increases gradually. (b) Dependence of the critical ratio on coupling strength ϵ and feedback parameter η. The colorbar indicates the value of critical ratio p_c.

of ϵ while $\eta = 0$. As can be seen, AT occurs at $p_c = 0.89$ (for $\epsilon = 3.0$) where the order parameter Z vanishes and the entire system gets stabilized to the trivial fixed point for $p \geqslant p_c$. However, with smaller $\epsilon = 2.0$, the transition appears only when all the nodes of network are made inactive, i.e., with $p_c = 1$. Also, for higher $\epsilon = 5.0$ and 7.0, the aging transition can be observed much earlier at $p_c = 0.8$ and 0.77, respectively. In fact, as the coupling strength ϵ increases, the critical inactivation ratio p_c decreases [12].

Now we will inspect the effects of introducing nonzero feedback strength η into the network for a fixed value of diffusive coupling strength ϵ. For this, we first choose a definite value of $\epsilon = 5.0$ and then see the diversity in the network dynamics by changing the feedback strength η. As shown earlier, p_c is found to be $p_c \approx 0.8$ when $\eta = 0$. But a minute increment in η to $\eta = 0.1$ revives the dynamical activity and hence enhances the network robustness to some extent, as p_c increases to $p_c = 0.82$ [see Fig. 3(a)]. As we increase the value of η to $\eta = 0.3$ and 0.5, the critical values p_c become $p_c = 0.87$ and 0.91, respectively. This indicates a significant improvement in the resilience of the network to progressive dynamical inactivation of the nodes. Even higher $\eta = 0.8$ leads the aging transition to occur at $p_c = 0.97$. Thus, for increasing η, the network is able to survive exhibiting global oscillation even when almost all the nodes are in inactive modes. For a better perception of this effect, next we plot the values of p_c in the ϵ-η parameter plane, as in Fig. 3(b). The positive influence of increasing η in resurgence of global oscillation for any ϵ (no matter how large) is conspicuous from the figure.

Now, to derive the critical value of the inactivation ratio analytically, we assume $z_j = A(j = 1,2,\ldots,N - Np)$ for active oscillators and $z_j = I(j = N - Np + 1,\ldots,N)$ for inactive oscillators. Then, from Eq. (3) with $\tau = 0$, the reduced coupled system becomes

$$\begin{aligned} \dot{A} &= (a + i\omega - \epsilon p + \eta q - |A|^2)A + (\epsilon + \eta)pI, \\ \dot{I} &= (-b + i\omega - \epsilon q + \eta p - |I|^2)I + (\epsilon + \eta)qA, \end{aligned} \tag{4}$$

where $q = 1 - p$. Now, as the aging transition corresponds to the stabilization of the trivial fixed point $A = I = 0$, we go through a linear stability analysis around the origin, that gives

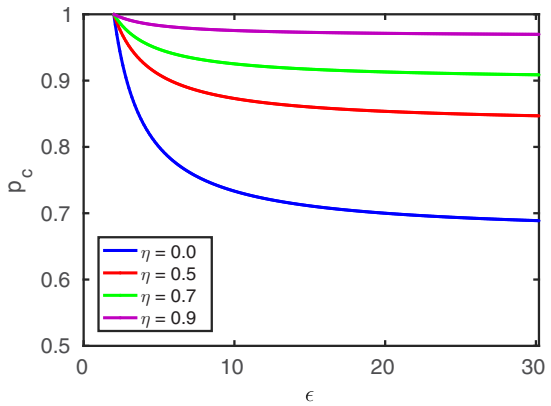

FIG. 4. The critical ratio p_c vs the coupling strength ϵ for different η values obtained from the analytical Eq. (5). The dynamical robustness of the system (1) enhances with increasing η.

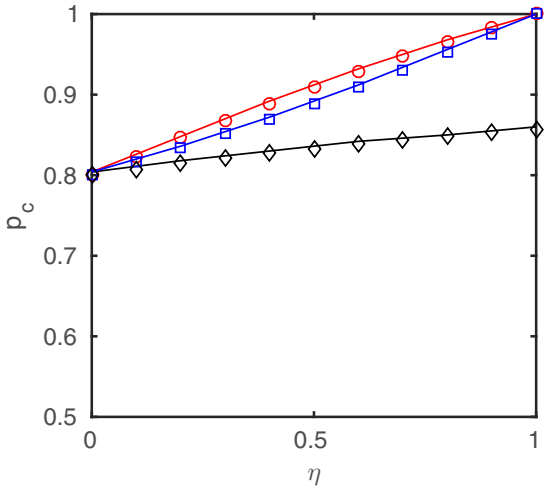

FIG. 5. The critical ratio p_c against the feedback parameter η for three different procedures of adding feedback to the network. Feedback is added to all the nodes (red), only to the inactive nodes (blue) and only to the active nodes (black). Here the coupling strength is fixed at $\epsilon = 5$.

the following Jacobian matrix:

$$\begin{pmatrix} a + i\omega - \epsilon p + \eta q & (\epsilon + \eta)p \\ (\epsilon + \eta)q & -b + i\omega - \epsilon q + \eta p \end{pmatrix}.$$

The negativity of real parts of all the eigenvalues of this matrix characterizes the stability of the origin ($A = I = 0$), investigation of which leads to the critical inactivation ratio p_c as

$$p_c = \frac{(a+\eta)(b+\epsilon)}{(\epsilon+\eta)(b+a)}, \tag{5}$$

with $\epsilon \geqslant \epsilon_c = a$. Of course, for the case with no feedback, $p_c = \frac{a(b+\epsilon)}{\epsilon(b+a)}$ is the same as in [12]. This value of p_c matches with the numerically calculated p_c for a,b,ϵ, and η taken so far while generating Figs. 2 and 3. The analytically obtained p_c [see Eq. (5)] with respect to increasing values of ϵ is figured out in Fig. 4 for several values of η. The blue curve signifies the p_c values against ϵ ($0 \leqslant \epsilon \leqslant 30$) whenever $\eta = 0$. Initially, p_c starts falling quite rapidly, but after certain $\epsilon \gtrsim 15$ this fall is rather insignificant. As expected, a similar sort of drop in p_c is observed whenever $\eta = 0.5$ is chosen (the curve in red), but more importantly this curve stays well above the previous one (in blue), indicating resumption of the dynamism in the network to a great extent irrespective of the interaction strength ϵ. For higher $\eta = 0.7$ and 0.9, the curves (respectively, in green and purple) depict even more enhancement in the network persistence. However, in all the cases after a certain ϵ, minimal changes in the value of p_c can be seen but AT is realized for any amount of coupling strength ϵ. This scenario is in contrast to the $p_c - \epsilon$ variation reported in [19], where AT was observed only for finite intervals of coupling strength.

As we are dealing with a mechanism of inducing external feedback in a blended network ensemble of active and inactive dynamical systems, one needs to scrutinize the impacts of different possible approaches of adding feedback to the network in detail. In order to do this, we plot the critical inactivation ratio p_c versus the feedback strength η while feedbacks are added to all the nodes, both active and inactive, in Fig. 5 (in red, circles are analytical results whereas the solid line corresponds to the numerical result). Since feedback is basically making the network more resilient (as discussed earlier), p_c values monotonically increase with increasing η ($0 \leqslant \eta \leqslant 1$). After that, we employ feedback only to the nodes in inactive mode, for which the reduced system becomes

$$\begin{aligned} \dot{A} &= (a + i\omega - \epsilon p - |A|^2)A + \epsilon p I, \\ \dot{I} &= (-b + i\omega - \epsilon q + \eta p - |I|^2)I + (\epsilon + \eta) q A, \end{aligned} \tag{6}$$

and there exists meager difference in the p_c values compared to the previous case. The analytical ($p_c = \frac{a(b+\epsilon)}{\epsilon(a+b)+\eta(a-\epsilon)}$) and numerical results [47] are, respectively, shown by blue squares and a solid line. This implies that it may be enough to apply feedback only to the inactive nodes in order to enhance the dynamical survivability in the network. At the time of giving feedback to the active group of nodes only, the reduced system becomes

$$\begin{aligned} \dot{A} &= (a + i\omega - \epsilon p + \eta q - |A|^2)A + (\epsilon + \eta) p I, \\ \dot{I} &= (-b + i\omega - \epsilon q - |I|^2)I + \epsilon q A. \end{aligned} \tag{7}$$

In this case, $p_c = \frac{(a+\eta)(b+\epsilon)}{\epsilon(a+b)+\eta(b+\epsilon)}$ shows increasing feedback strength, η makes the network more robust but not as much as in the preceding two cases. The black diamonds and the solid line are below the red and blue ones, as in Fig. 5. This study helps one to perceive the way one should embed the feedback function in the system.

B. Time-delayed interaction and feedback

It is the purpose of this subsection to inspect what feedback does whenever there is time delay in the diffusive interaction among the globally coupled nodes. According to the results addressed in [16], p_c decreases for increasing values of τ, that readily suggests a deenhancing tendency of delay, in the absence of the feedback term. As reported in the previous subsection, for a fixed coupling strength $\epsilon = 5$ and feedback strength $\eta = 0$, without delay τ, the value of p_c happens to be $p_c = 0.8$. But as delay $\tau = 0.5$ is incorporated in the system p_c decreases to $p_c = 0.63$, as displayed in Fig. 6(a). Remarkably, if η is now introduced in the network, it becomes more resilient, which can be easily discernible from the values of

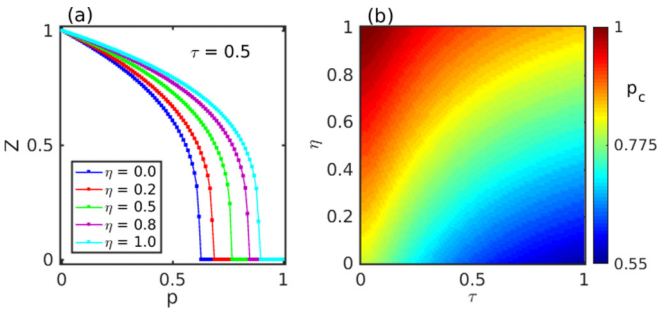

FIG. 6. (a) The order parameter Z against the inactivation ratio p for various η values in the delay coupled network (3) with $N = 500$, $\tau = 0.5$, and $\epsilon = 5$. (b) Dependence of the value of critical ratio p_c on $\eta - \tau$ parameter space.

$p_c = 0.69$ and 0.77, respectively, for $\eta = 0.2$ and 0.5. Higher $\eta = 0.8$ and 1.0 are perfectly able to resume dynamical activity in the form of global oscillation to a greater extent as p_c turns into $p_c = 0.85$ and 0.9, respectively, as depicted in Fig. 6(a). Moreover, the impact of η is illustrated for a sufficiently long range of the delay $\tau \in [0,1]$ in Fig. 6(b), that readily describes the enhancing effect of increasing η for any value of τ. Thus as observed in the instantaneous interaction scheme, here again η is developing the network survivability altogether even in the presence of time delay in the coupling.

On the other hand, following a similar approach as in the previous case for globally coupled oscillators, the reduced model for active and inactive oscillators in the case of time-delayed interaction with feedback mechanism becomes

$$\begin{aligned}\dot{A}(t) &= \left[a + i\omega - \epsilon\left(1 - \frac{1}{N}\right) - |A(t)|^2 + \eta q\right]A(t) \\ &\quad + \eta p I(t) + \epsilon\left(q - \frac{1}{N}\right)A(t-\tau) + \epsilon p I(t-\tau), \\ \dot{I}(t) &= \left[-b + i\omega - \epsilon\left(1 - \frac{1}{N}\right) - |I(t)|^2 + \eta p\right]I(t) \\ &\quad + \eta q A(t) + \epsilon\left(p - \frac{1}{N}\right)I(t-\tau) + \epsilon q A(t-\tau). \quad (8)\end{aligned}$$

From linear stability analysis of Eq. (8) around the origin and setting the real part of the eigenvalue equal to zero, we obtain the characteristic equation for eigenvalues as

$$\begin{aligned}&\left[a - \epsilon\left(1 - \frac{1}{N}\right) + i(\omega - \lambda_I) + \eta q + \epsilon\left(q - \frac{1}{N}\right)e^{-i\lambda_I\tau}\right] \\ &\times\left[-b - \epsilon\left(1 - \frac{1}{N}\right) + i(\omega - \lambda_I) + \eta p\right. \\ &\left. + \epsilon\left(p - \frac{1}{N}\right)e^{-i\lambda_I\tau}\right] - pq(\eta + \epsilon e^{-i\lambda_I\tau})^2 = 0, \quad (9)\end{aligned}$$

where λ_I is the imaginary part of the eigenvalue λ, i.e., $\lambda = i\lambda_I$. Separating real and imaginary parts we get the following equations:

$$\begin{aligned}&[\omega - \lambda_I - B\sin(\lambda_I\tau)][\omega - \lambda_I - C\sin(\lambda_I\tau)] \\ &\quad - [g_1 + g_3 + B\cos(\lambda_I\tau)][g_2 + g_4 + C\cos(\lambda_I\tau)] \\ &\quad = -g_3 g_4 - D_1\cos(\lambda_I\tau) - D_2\cos(2\lambda_I\tau), \quad (10)\end{aligned}$$

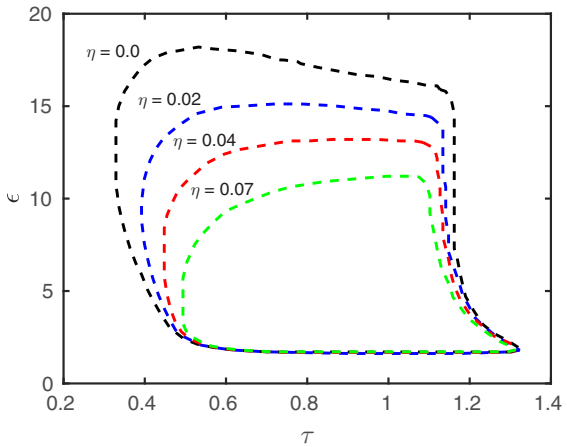

FIG. 7. Aging islands in the $\epsilon - \tau$ parameter plane at different values of the feedback parameter η for fixed inactivation ratio $p = 0.65$. Here the size of the aging islands reduces significantly with the increase of η value.

$$\begin{aligned}&[\omega - \lambda_I - B\sin(\lambda_I\tau)][g_2 + g_4 + C\cos(\lambda_I\tau)] \\ &\quad + [\omega - \lambda_I - C\sin(\lambda_I\tau)][g_1 + g_3 + B\cos(\lambda_I\tau)] \\ &\quad = -D_1\sin(\lambda_I\tau) - D_2\sin(2\lambda_I\tau), \quad (11)\end{aligned}$$

where $g_1 = a - \epsilon(1 - \frac{1}{N}), B = \epsilon(q - \frac{1}{N}), g_2 = -b - \epsilon(1 - \frac{1}{N}), C = \epsilon(p - \frac{1}{N}), g_3 = \eta q, g_4 = \eta p, D_1 = 2\eta\epsilon pq,$ and $D_2 = \epsilon^2 pq$.

Figure 7 depicts the aging islands in the ϵ-τ parameter plane obtained from the set of equations (10) and (11) for different values of the feedback strength η. For a fixed inactivation ratio $p = 0.65$, first the aging island is plotted (in black) whenever $\eta = 0$. Next the same is displayed for $\eta = 0.02$ (in blue) in Fig. 7. It is easily observed that the aging island in the parameter plane gets reduced significantly for this nonzero η, that readily implies enhancement in the network's dynamical persistence. Further increment in η to $\eta = 0.04$ and 0.07 (in red and green, respectively) helps in shortening the aging island area more comprehensively.

IV. INTERACTION ON COMPLEX NETWORKS

This section is devoted to the discussion of efficiency of the external feedback function on developing dynamical robustness in a network possessing complex interactional topologies. Particularly, we will be analyzing this scenario on top of both small-world and scale-free architectures.

A. Small-world interaction

Small-world networks [48] appear as a result of random rewiring of links (with a certain probability p_{SW}) in a regular (lattice) network, interpolating between two limiting cases of regular ($p_{SW} = 0$) and random ($p_{SW} = 1$) topologies that maintain low diameter and high clustering coefficient in the network.

Choosing $N = 500$, $p_{SW} = 0.01$ and the link density $d = \langle k\rangle/(N-1) = 0.24$ ($\langle k\rangle$ being the average degree of the

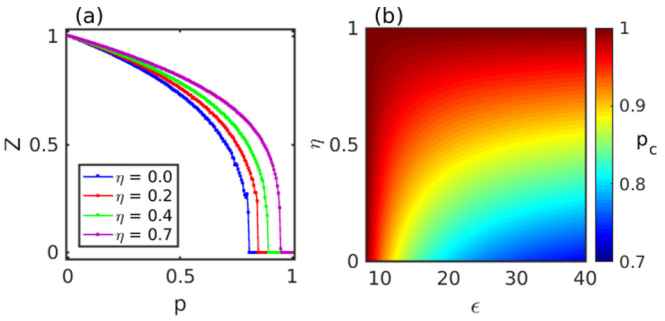

FIG. 8. Effect of feedback parameter on small-world network: (a) the order parameter Z against the inactivation ratio p for various η values in small-world network with $d = 0.24$ and coupling strength $\epsilon = 20$ and (b) dependence of the critical ratio p_c in $\epsilon - \eta$ parameter space.

nodes). Figure 8(a) shows variation in the order parameter Z against p for $\eta = 0,0.2,0.4$, and 0.7 while the oscillators are interacting over a small-world topology. In the absence of feedback, Z declines to zero at $p_c = 0.805$, indicating aging transition for coupling strength $\epsilon = 20$. But p_c value increases to $p_c = 0.85$ and 0.892, respectively, with $\eta = 0.2$ and 0.4 signifying improvement in the network survivability. Whenever $\eta = 0.7$, the network becomes more resilient as it turns out to be able to retain dynamism even up to $p = 0.95$.

Next we analytically derive the critical ratio p_c for random inactivation in a small-world network in the presence of the feedback parameter η. The reduced model for active and inactive oscillators in the case of a small-world network with feedback parameter η can be written as

$$\begin{aligned} \dot{A} &= (a + i\omega - \epsilon dp + \eta q - |A|^2)A + (\epsilon d + \eta)pI, \\ \dot{I} &= (-b + i\omega - \epsilon dq + \eta p - |I|^2)I + (\epsilon d + \eta)qA, \end{aligned} \tag{12}$$

as the number of inactive oscillators in the neighborhood of each oscillator is expected to be $p\langle k\rangle$ and that of the active oscillators is $(1-p)\langle k\rangle$, where $q = 1 - p$ and $d = \langle k\rangle/N - 1$ is the link density of the network. From the linear stability analysis around the fixed point $A = I = 0$, we get the critical inactivation ratio p_c as

$$p_c = \frac{(a+\eta)(b+\epsilon d)}{(\epsilon d+\eta)(b+a)}, \tag{13}$$

with $\epsilon \geqslant \epsilon_c = a/d$.

Having this value of the critical inactivation ratio p_c [see Eq. (13)], we plot its dependence on simultaneous variation of the coupling strength $\epsilon \in [8,40]$ and feedback parameter $\eta \in [0,1]$ for a small-world network in Fig. 8(b). From the figure, it is quite conspicuous that the higher the feedback strength the more the network is dynamically persistent, irrespective of the strength of interaction ϵ.

B. Scale-free interaction

On the other hand, a scale-free architecture [49] corresponds to a highly heterogeneous scenario as far as the degree distribution is concerned, that basically follows a power law $P(k) \sim k^{-\gamma}$, where $P(k)$ is the probability of finding a node of degree k and γ is the power-law exponent (in our case, $\gamma = 3.0$). First we concentrate on how the degree-weighted mean-field approach yields a good approximation for the

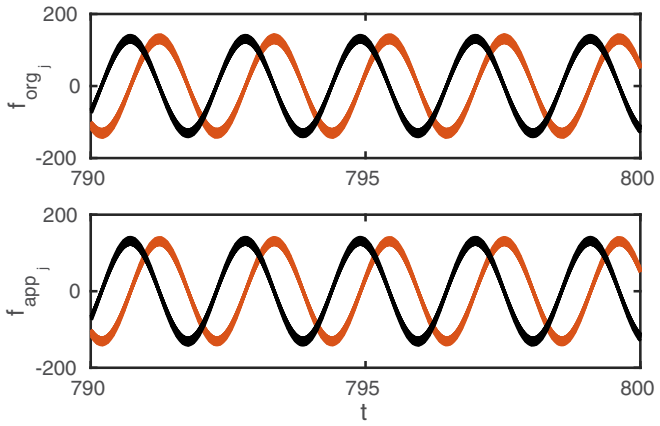

FIG. 9. Validation of the original fields f_{org_j} by the approximated mean fields f_{app_j} considering $N = 500, d = 0.078, \epsilon = 80$, and $p = 0.5$. The upper panel shows the original local fields of several oscillators while the lower panel shows the corresponding approximated fields. Here black and brown color, respectively, corresponds to the real and imaginary parts of the local fields.

original local fields associated to the scale-free architecture, the process that we will be mainly following in order to analytically estimate the critical ratio p_c. According to the degree-weighted mean field approximation [50], the original local field f_{org_j} can be approximated by f_{app_j} as

$$\begin{aligned} f_{\text{org}_j} &= \sum_{k=1}^{N} A_{jk} z_k \simeq (1-p)k_j H_A(t) \\ &\quad + pk_j H_I(t) = f_{\text{app}_j}, \end{aligned} \tag{14}$$

where $H_A(t) = \frac{\sum_{j\in S_A} k_j z_j(t)}{\sum_{j\in S_A} k_j}$ and $H_I(t) = \frac{\sum_{j\in S_I} k_j z_j(t)}{\sum_{j\in S_I} k_j}$ are the degree-weighted mean fields for active and inactive groups of dynamical units, respectively, and $k_j (j = 1,2,\ldots,N)$ is the degree of the jth node. Here S_A and S_I are the sets of all active and inactive nodes, respectively. Though the scale-free network is highly heterogeneous as far as the degree distribution is concerned, since we are actually dealing with degree-weighted mean fields $H_A(t)$ and $H_I(t)$ that involve a normalization through the degrees, this mean-field approach f_{app_j} yields quite a good approximation for the local fields f_{org_j} arising from a scale-free dynamical network. We justify this claim in Fig. 9 while plotting the approximated results of several oscillators through the mean-field approach that matches the original local fields.

Now we numerically study this transition for a scale-free network of $N = 500$ oscillators and $d = 0.078$. As can be observed from Fig. 10(a), with a fixed interaction strength $\epsilon = 200$ and no feedback, the order parameter drops down to zero for $p \geqslant p_c = 0.723$. Importantly enough, with a nonzero feedback $\eta = 0.2$, the value of p_c increases to $p_c = 0.782$. In a similar fashion, higher feedback strengths $\eta = 0.5$ and 0.8 lead to highly improved critical inactivation ratios $p_c = 0.867$ and 0.95, respectively. These outcomes are the indicators of resumption of dynamism in damaged complex networks of active and inactive units.

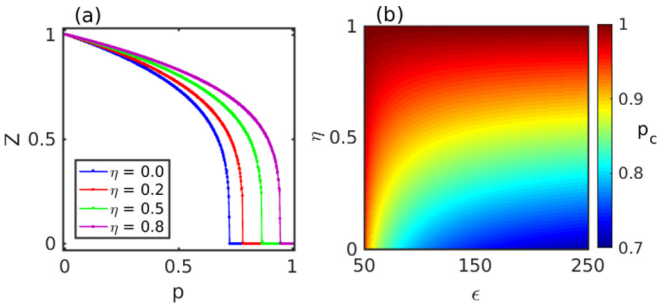

FIG. 10. Effect of feedback parameter in scale-free networks: (a) the order parameter Z against the inactivation ratio p for various η values in scale-free network with $\epsilon = 200$ and (b) dependence of the critical ratio p_c in $\epsilon - \eta$ parameter space.

According to Eq. (14), the original system (1) can be approximated as

$$\dot{z_j} = (\alpha + i\omega - |z_j|^2)z_j + \frac{\epsilon k_j}{N}[(1-p)H_A(t) + pH_I(t) - z_j] + \eta[(1-p)H_A(t) + pH_I(t)]. \quad (15)$$

Assuming that the state variables can be written as $z_j(t) = r_j(t)e^{i(\omega t+\theta)}$, where r_j is the amplitude and θ is the phase shift, and substituting it in Eq. (15) we obtain

$$\dot{r_j} = \left(\alpha - \frac{\epsilon k_j}{N} - r_j^2\right)r_j + \left(\frac{\epsilon k_j}{N} + \eta\right) \times [(1-p)R_A(t) + pR_I(t)], \quad (16)$$

where $R_A(t) = \frac{\sum_{j\in S_A} k_j r_j(t)}{\sum_{j\in S_A} k_j}$ and $R_I(t) = \frac{\sum_{j\in S_I} k_j r_j(t)}{\sum_{j\in S_I} k_j}$. Assuming the time independence of $R_A(t)$ and $R_I(t)$ in the stationary oscillatory regime, the phase transition from oscillatory $(R_A, R_I > 0)$ to nonoscillatory $(R_A = R_I = 0)$ takes place due to the change in stability of the fixed point at the origin. The stability is determined by the following Jacobian matrix:

$$J_0 = \left(\begin{array}{cc} \frac{\partial G_A(R_A,R_I)}{\partial R_A} & \frac{\partial G_A(R_A,R_I)}{\partial R_I} \\ \frac{\partial G_I(R_A,R_I)}{\partial R_A} & \frac{\partial G_I(R_A,R_I)}{\partial R_I} \end{array}\right)\Bigg|_{R_A=R_I=0},$$

where

$$G_A(R_A,R_I) = \frac{\sum_{j\in S_A} k_j r_j^*(R_A,R_I)}{\sum_{j\in S_A} k_j}, \qquad G_I(R_A,R_I) = \frac{\sum_{j\in S_I} k_j r_j^*(R_A,R_I)}{\sum_{j\in S_I} k_j} \quad (17)$$

and the stationary amplitude r_j^* is given by a positive real solution of the following equation:

$$r_j^3 - \left(\alpha_j - \frac{\epsilon k_j}{N}\right)r_j - \left(\frac{\epsilon k_j}{N} + \eta\right)[(1-p)R_A + pR_I] = 0. \quad (18)$$

Equation (18) has only one positive real root if we assume $\alpha_j - \frac{\epsilon k_j}{N} < 0$ for all $j \in S_A$. Differentiating Eqs. (17) and (18) with respect to R_A we obtain the first entry of J_0 as follows:

$$\frac{\partial G_A}{\partial R_A}\Big|_{R_A=R_I=0} = \frac{(1-p)\epsilon}{\sum_{j\in S_A} k_j}\left(\frac{1}{N}\sum_{j\in S_A}\frac{k_j^2}{\epsilon k_j/N - \alpha_j}\right) + \frac{(1-p)\eta}{\sum_{j\in S_A} k_j}\left(\frac{1}{N}\sum_{j\in S_A}\frac{k_j}{\epsilon k_j/N - \alpha_j}\right) \simeq \frac{1}{d}\left(\frac{1}{N}\sum_{j\in S_A}\frac{d_j^2}{d_j - \alpha_j/\epsilon}\right) + \frac{\eta}{d\epsilon}\left(\frac{1}{N}\sum_{j\in S_A}\frac{d_j}{d_j - \alpha_j/\epsilon}\right), \quad (19)$$

where $d_j = k_j/N$ is the ratio of the degree of the jth oscillator and the system size, and $d = \langle k\rangle/(N-1)$ is the link density of the network. Here the following approximations hold in the limit $N \to \infty$:

$$\sum_{j\in S_A} k_j \simeq (1-p)dN^2, \quad \sum_{j\in S_I} k_j \simeq pdN^2, \quad \frac{1}{N}\sum_{j\in S_A}\frac{d_j^2}{d_j - \alpha_j/\epsilon} \simeq (1-p)F(\epsilon,a),$$
$$\frac{1}{N}\sum_{j\in S_I}\frac{d_j^2}{d_j - \alpha_j/\epsilon} \simeq pF(\epsilon,-b), \quad \frac{1}{N}\sum_{j\in S_A}\frac{d_j}{d_j - \alpha_j/\epsilon} \simeq (1-p)\bar{F}(\epsilon,a)$$
$$\frac{1}{N}\sum_{j\in S_I}\frac{d_j}{d_j - \alpha_j/\epsilon} \simeq p\bar{F}(\epsilon,-b),$$

where

$$F(\epsilon,\alpha) \simeq \frac{1}{N}\sum_{j=1}^{N}\frac{d_j^2}{d_j - \alpha/\epsilon}, \quad \bar{F}(\epsilon,\alpha) \simeq \frac{1}{N}\sum_{j=1}^{N}\frac{d_j}{d_j - \alpha/\epsilon}.$$

Therefore we obtain

$$J_0 = \left(\begin{array}{cc} \frac{(1-p)}{d}[F(\epsilon,a) + \frac{\eta}{\epsilon}\bar{F}(\epsilon,a)] & \frac{p}{d}[F(\epsilon,a) + \frac{\eta}{\epsilon}\bar{F}(\epsilon,a)] \\ \frac{(1-p)}{d}[F(\epsilon,-b) + \frac{\eta}{\epsilon}\bar{F}(\epsilon,-b)] & \frac{p}{d}[F(\epsilon,-b) + \frac{\eta}{\epsilon}\bar{F}(\epsilon,-b)] \end{array}\right).$$

The fixed point changes its stability at the phase transition point at $R_A = R_I = 0$, which compels us to obtain the following critical inactivation ratio:

$$p_c = \frac{F(\epsilon,a) + \frac{\eta}{\epsilon}\bar{F}(\epsilon,a) - d}{[F(\epsilon,a) - F(\epsilon,-b)] + \frac{\eta}{\epsilon}[\bar{F}(\epsilon,a) - \bar{F}(\epsilon,-b)]}, \tag{20}$$

for $\epsilon > \epsilon_c(= a/d_{\min})$, where $d_{\min} = k_{\min}/N$. Particularly, for $\eta = 0$, i.e., when there is no feedback in the system, the critical inactivation ratio becomes

$$p_c = \frac{F(\epsilon,a) - d}{F(\epsilon,a) - F(\epsilon,-b)}.$$

We also plot the critical ratio p_c [see Eq. (20)] as a function of $\epsilon \in [50,250]$ and $\eta \in [0,1]$ for scale-free configuration of the network in Fig. 10(b) with the same network and system parameters used for the numerical simulations. Analytically found critical values perfectly match the numerical ones, and external feedback has been observed to develop dynamical survivability throughout all values of ϵ.

V. EFFECT OF FEEDBACK ON INTERACTING RÖSSLER SYSTEMS

Finally, we examine the effectiveness of our approach while choosing a chaotic dynamical system coupled through both regular (global) and complex topologies. The mathematical form of the damaged network of N interacting delay coupled Rössler systems is as follows:

$$\begin{aligned}
\dot{x}_j &= -y_j - z_j + \frac{\epsilon}{N}\sum_{k=1,k\neq j}^{N} A_{jk}[x_k(t-\tau) - x_j] + \frac{\eta}{N}\sum_{k=1}^{N} x_k,\\
\dot{y}_j &= x_j + c_j y_j + \frac{\epsilon}{N}\sum_{k=1,k\neq j}^{N} A_{jk}[y_k(t-\tau) - y_j] + \frac{\eta}{N}\sum_{k=1}^{N} y_k,\\
\dot{z}_j &= d_j + z_j(x_j - e_j) + \frac{\epsilon}{N}\sum_{k=1,k\neq j}^{N} A_{jk}[z_k(t-\tau) - z_j]\\
&\quad + \frac{\eta}{N}\sum_{k=1}^{N} z_k,
\end{aligned} \tag{21}$$

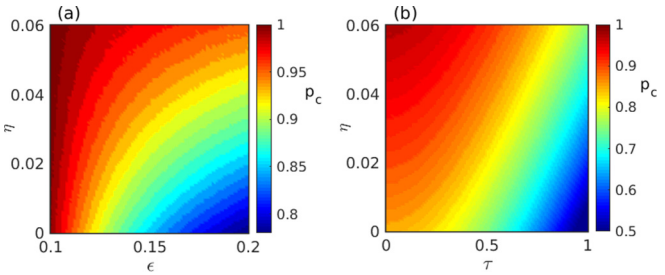

FIG. 11. Dependence of the critical ratio p_c on (a) $\epsilon - \eta$ parameter space for nondelayed interaction ($\tau = 0$) and (b) $\tau - \eta$ parameter space for delayed interaction with fixed coupling strength $\epsilon = 0.15$ in a network of $N = 500$ globally coupled chaotic Rössler oscillators.

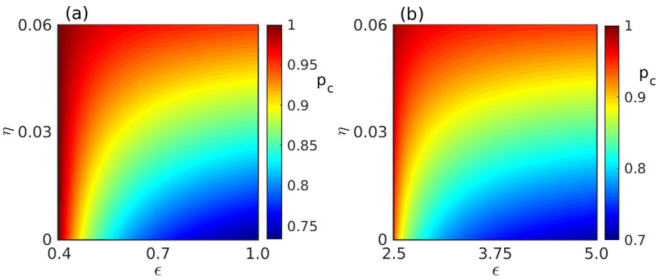

FIG. 12. Dependence of the critical ratio p_c on coupling strength ϵ and feedback parameter η considering (a) small-world and (b) scale-free network of $N = 500$ coupled chaotic Rössler oscillators.

for $j = 1,2,\ldots,N$. Here $c_j = d_j = 0.2$, $e_j = 5.7$ for the active (chaotic) group of oscillators and $c_j = d_j = -0.2$, $e_j = 2.5$ for inactive oscillators.

We start with defining the order parameter M as $M = \sqrt{\langle(\mathbf{X}_c - \langle\mathbf{X}_c\rangle)^2\rangle}$, where $\mathbf{X}_c = \frac{1}{N}\sum_{j=1}^{N}(x_j,y_j,z_j)$ is the centroid and the bracket $\langle\ldots\rangle$ means a long time average. Aging transition of the system (21) is further described in terms of this M.

Figure 11(a) depicts change in p_c for the nondelayed case, i.e., $\tau = 0$, with respect to simultaneous variation in the coupling strength $\epsilon \in [0.1,0.2]$ and feedback strength $\eta \in [0,0.06]$. Whenever $\eta = 0$, p_c gradually decreases for increasing ϵ and reaches $p_c \simeq 0.78$ for $\epsilon = 0.2$. But, as we employ a feeble increment in η, it starts raising this critical value of p greatly even to $p_c \simeq 0.95$ for $\eta = 0.06$. This scenario is valid for any value of ϵ, implying significant improvement in the network resilience. The impact of η in the case of delay coupled oscillators is also illustrated in Fig. 11(b) for time delay $\tau \in [0,1]$. Moreover, to corroborate the generality of our approach, in Fig. 12 we unveil the effect of feedback parameter η on a network of coupled chaotic Rössler oscillators with small-world and scale-free topologies. Figure 12(a) portrays the dependence of the critical ratio p_c on simultaneous variation of the coupling strength $\epsilon \in [0.4,1]$ and the feedback strength $\eta \in [0,0.06]$ in a small-world network with rewiring probability $p_{SW} = 0.01$ and link density $d = 0.24$, whereas Fig. 12(b) depicts the result for variations of $\epsilon \in [2.5,5]$ and $\eta \in [0,0.06]$ in a scale-free network with link density $d = 0.078$. Noticeably, for both these architectures, the applied feedback enhances the network survivability against badness of the dynamical units. This is how the proposed mechanism of enhancing survivability for time-delayed and complex networks works whenever chaotic systems are used to cast the active units in the damaged network.

VI. CONCLUSIONS

Network robustness has recently become a topic of great research interest because it bears resemblance to various natural occurrences. In the present paper, we have gone through the notion of rescuing networks from a comprehensive collapse due to a specific type of dynamical perturbation. Particularly, we have examined the dynamical robustness of damaged networks in terms of aging transition and demonstrated how one can resume dynamism through a feedback mechanism. We have shown that by simply adding an appropriate linear

feedback term in the aging network the network's survivability can be developed quite substantially. This enhancing impact of the feedback is observed to be effective irrespective of the coupling strength. We have illustrated this scenario through both numerical and analytical findings while considering limit cycle Stuart-Landau systems as the local dynamical units. A comparative study on the process of adding feedbacks to only active, only inactive, and both active and inactive groups of nodes has also been presented. Notably, we have been able to develop network persistence even in the presence of time delay in the interaction among the nodes, although delay is a candidate that may effectively lower the network resilience. As far as the generalization of our approach over different network topologies is concerned, we have realized the same qualitative features of external feedback in small-world as well as scale-free complex structures of the aging networks. In order to reveal the local system independence of our scheme, we successfully performed similar analysis for chaotic Rössler oscillators. Our paper may have important applications in increasing the survivability of several natural systems that experience local inactivation of their components.

ACKNOWLEDGMENTS

The authors are grateful to the anonymous referee for insightful comments, that helped in improving the paper. D.G. was supported by the Department of Science and Technology, Government of India (Project No. EMR/2016/001039).

[1] A. Pikovsky, M. Rosenblum, and J. Kurths, *Synchronization: A Universal Concept in Nonlinear Sciences* (Cambridge University, Cambridge, England, 2004).
[2] S. H. Strogatz, *Sync: How Order Emerges From Chaos In the Universe, Nature, and Daily Life* (Hyperion, New York, 2004).
[3] R. Albert, H. Jeong, and A.-L. Barabasi, Nature (London) **406**, 378 (2000).
[4] R. Cohen, K. Erez, D. ben-Avraham, and S. Havlin, Phys. Rev. Lett. **85**, 4626 (2000).
[5] P. Crucitti, V. Latora, M. Marchiori, and A. Rapisarda, Physica A (Amsterdam) **320**, 622 (2003).
[6] S. V. Buldyrev, R. Parshani, G. Paul, H. E. Stanley, and S. Havlin, Nature (London) **464**, 1025 (2010).
[7] S. N. Dorogovtsev, A. V. Goltsev, and J. F. F. Mendes, Rev. Mod. Phys. **80**, 1275 (2008).
[8] A. Vespignani, Nature (London) **464**, 984 (2010).
[9] S.-W. Son, G. Bizhani, C. Christensen, P. Grassberger, and M. Paczuski, Europhys. Lett. **97**, 16006 (2012).
[10] J. Gao, X. Liu, D. Li, and S. Havlin, Energies **8**, 12187 (2015).
[11] J. Gao, B. Barzel, and A.-L. Barabási, Nature (London) **530**, 307 (2016).
[12] H. Daido and K. Nakanishi, Phys. Rev. Lett. **93**, 104101 (2004).
[13] H. Daido and K. Nakanishi, Phys. Rev. E **75**, 056206 (2007).
[14] H. Daido, Phys. Rev. E **83**, 026209 (2011).
[15] K. Morino, G. Tanaka, and K. Aihara, Phys. Rev. E **83**, 056208 (2011).
[16] B. Thakur, D. Sharma, and A. Sen, Phys. Rev. E **90**, 042904 (2014).
[17] G. Tanaka, K. Morino, and K. Aihara, Sci. Rep. **2**, 232 (2012).
[18] K. Morino, G. Tanaka, and K. Aihara, Phys. Rev. E **88**, 032909 (2013).
[19] Y. Liu, W. Zou, M. Zhan, J. Duan, and J. Kurths, Europhys. Lett. **114**, 40004 (2016).
[20] Z. Sun, N. Ma, and W. Xu, Sci. Rep. **7**, 42715 (2017).
[21] E. Ranta, M. S. Fowler, and V. Kaitala, Proc. R. Soc. B **275**, 435 (2008).
[22] L. J. Gilarranz and J. Bascompte, J. Theor. Biol. **297**, 11 (2012).
[23] S. Kundu, S. Majhi, S. K. Sasmal, D. Ghosh, and B. Rakshit, Phys. Rev. E **96**, 062212 (2017).
[24] J. Lisman and G. Buzsáki, Schizophrenia Bulletin **34**, 974 (2008).
[25] J. Jalife, R. A. Gray, G. E. Morley, and J. M. Davidenko, Chaos **8**, 79 (1998).
[26] W. L. Koukkari and R. B. Sothern, *Introducing Biological Rhythms: A Primer on the Temporal Organization of Life, with Implications for Health, Society, Reproduction, and the Natural Environment* (Springer, New York, 2007).
[27] G. C. Gurtner, M. J. Callaghan, and M. T. Longaker, Annu. Rev. Med. **58**, 299 (2007).
[28] A. Buscarino, L. V. Gambuzza, M. Porfiri, L. Fortuna, and M. Frasca, Sci. Rep. **3**, 2026 (2013).
[29] L. V. Gambuzza, A. Buscarino, L. Fortuna, M. Porfiri, and M. Frasca, IEEE J. Emerg. Sel. Topics Circuits Syst. **7**, 413 (2017).
[30] G. Franklin, J. Powell, and A. E.-Naeini, *Feedback Control of Dynamic Systems*, 2nd ed. (Addison-Wesley, Reading, MA, 1991).
[31] K. J. Åström and R. M. Murray, *Feedback Systems: An Introduction for Scientists and Engineers* (Princeton University, Princeton, NJ, 2008).
[32] D. L. DeAngelis, W. M. Post, and C. C. Travis, *Positive Feedback in Natural Systems*, Biomathematics Vol. 15 (Springer, New York, 1986).
[33] A. Becskei, B. Séraphin, and L. Serrano, Embo. J. **20**, 2528 (2001).
[34] Y.-T. Huang, Y.-L. Chang, C.-C. Chen, P.-Y. Lai, and C. K. Chan, PLoS ONE **12**, e0187276 (2016).
[35] S. C. Kak, Circuits, Systems and Signal Processing **12**, 263 (1993).
[36] M. G. Rosenblum and A. S. Pikovsky, Phys. Rev. Lett. **92**, 114102 (2004).
[37] O. V. Popovych, C. Hauptmann, and P. A. Tass, Phys. Rev. Lett. **94**, 164102 (2005).
[38] V. K. Chandrasekar, J. H. Sheeba, and M. Lakshmanan, Chaos **20**, 045106 (2010).
[39] V. Semenov, A. Feoktistov, T. Vadivasova, E. Schöll, and A. Zakharova, Chaos **25**, 033111 (2015).
[40] T. E. Murphy *et al.*, Philos. Trans. R. Soc. London A **368**, 343 (2010).

[41] V. K. Chandrasekar, S. Karthiga, and M. Lakshmanan, Phys. Rev. E **92**, 012903 (2015).
[42] K. Yadav, N. K. Kamal, and M. D. Shrimali, Phys. Rev. E **95**, 042215 (2017).
[43] V. A.-Lodi, S. Donati, and A. Sciré, IEEE J. Quantum Electron. **33**, 1449 (1997).
[44] H. Ando, K. Takehara, and M. U. Kobayashi, Phys. Rev. E **96**, 012148 (2017).
[45] B. K. Bera, D. Ghosh, P. Parmananda, G. V. Osipov, and S. K. Dana, Chaos **27**, 073108 (2017).
[46] The fifth-order Runge-Kutta Fehlberg scheme and modified Heun method have been used to integrate the nondelayed and delayed dynamical equations, respectively.
[47] The numerical results are calculated using the same order parameter as defined in Sec. II.
[48] D. J. Watts and S. H. Strogatz, Nature (London) **393**, 440 (1998).
[49] A.-L. Barabási and R. Albert, Science **286**, 509 (1999).
[50] R. Pastor-Satorras and A. Vespignani, Phys. Rev. Lett. **86**, 3200 (2001).